



## Heat Transfer of A Peristaltic Electro - Osmotic Flow of A Couple Stress Fluid through an Inclined Asymmetric Channel with Effects of Thermal Radiation

K. Venugopal Reddy<sup>1\*</sup>, Mantha Srikanth<sup>2</sup> and K. Ramakrishna Reddy<sup>3</sup>

<sup>1</sup>Associate Professor, Department of Mathematics, Malla Reddy Engineering College (Autonomous), Maisammaguda, Hyderabad, Telangana, India.

<sup>2</sup>Assistant Professor, Department of Mathematics, Malla Reddy Engineering College (Autonomous), Maisammaguda, Hyderabad, Telangana, India.

<sup>3</sup>Professor, Department of Mathematics, Malla Reddy Engineering College (Autonomous), Maisammaguda, Hyderabad, Telangana, India.

Received: 02 Sep 2022

Revised: 20 Oct 2022

Accepted: 23 Nov 2022

### \*Address for Correspondence

**K. Venugopal Reddy**

Associate Professor,  
Department of Mathematics,  
Malla Reddy Engineering College (Autonomous),  
Maisammaguda, Hyderabad, Telangana, India.  
Email: venugopal.reddy1982@gmail.com



This is an Open Access Journal / article distributed under the terms of the **Creative Commons Attribution License** (CC BY-NC-ND 3.0) which permits unrestricted use, distribution, and reproduction in any medium, provided the original work is properly cited. All rights reserved.

### ABSTRACT

The presented article addresses the electro-osmotic peristaltic flow of a couple-stress fluid bounded in an inclined asymmetric micro-channel. The viscous dissipation, Joule heating and chemical reaction effects are employed simultaneously in the flow analysis. Heat and mass transfer have been studied under large wave length and small Reynolds number. The resulting nonlinear systems are solved numerically. The influence of various dominant physical parameters is discussed for velocity, temperature distribution, and the pumping characteristics.

**Keywords:** Peristaltic flow; Electro-osmotic flow; Couple stress fluid; Magnetic field; Heat transfer; Mass transfer; Inclined asymmetric micro-channel;

### INTRODUCTION

Recent investigations in miniaturization and micro-fabrication have taken into assuming a lot of applications extending from organic to refrigerating of microelectronics in [1 - 9]. Many favors such as an important reduction in the utilization of required materials, ability to achieve in-vitro experiments on the continuous motion in a manner





**Venugopal Reddy et al.,**

similar to the real situation in a living biological system, being portable and vibration-free are using micro fluidic devices. Electro-osmotic transports with thermal effects of liquids in micro channels are reported in [10]. The heat transfer investigation of electro-osmotic motion in a slowly varying non-symmetric micro-channel is presented in [11]. Stokes developed the couple stress fluid model. When additives are mixed in the fluid then cohesive forces of fluid resists additive factors. This resistance creates a combined force and then a couple stress is generated in the fluid. Such fluid is known as couple stress fluid. This model is regarded as generalization of Newtonian fluid model dealing with body couples and couple stresses in fluid medium. Note that couple stress fluid has an asymmetric stress tensor. Relevant studies in this direction are given in the investigations [12 – 18]. Bio-fluids propel from one place to another place by continuous process of muscle contraction and relaxation. This process is known as peristaltic transport. The peristaltic transport phenomenon is mainly due to the neuromuscular property of any tubular smooth muscle structure. This mechanism is responsible for the transport of biological fluids in several physiological processes such as urine transport from kidney to the bladder, the movement of chyme into the gastrointestinal tract, fluids in the lymphatic vessels, bile from the gallbladder into the duodenum, the embryo transport in non-pregnant uterus, the movement of spermatozoa in the ducts efferent of the male reproductive tract, the movement of the ovum in the fallopian tube and the circulation of blood in small blood vessels are depicted in [19 – 33]. Thus the major focus of this study is to analyze the viscous dissipation, Joule heating effects on MHD electro-osmotic peristaltic flow of couple stress fluid in an inclined asymmetric micro channel. Mathematical formulation of problem is presented. The results are obtained after employing long wavelength and low Reynolds number approximation. The velocity, temperature, concentration, pressure gradient and pressure rise have been proposed for the pertinent parameters of interest.

**Mathematical Formulation and analysis**

We analyze the electro-osmotic peristaltic flow of an electrically conducting incompressible couple stress fluid and heat transfers through an inclined asymmetric micro-channel with charged walls under the influence of an imposed the magnetic field. The flow is assumed to be asymmetric about  $x'$  and the liquid is flowing in the  $x'$ -direction. The hydrophobic micro-channel is bounded by slowly varying walls at  $y' = h_1(x')$  and  $y' = h_2(x')$  respectively, in which the length of the channel ( $L$ ) is assumed to be much larger than the height, i.e.,  $L \gg (h_1 + h_2)$ . Fig. 1 below depicts the schematic diagram of the problem under current study.

**Electrical Potential Distribution**

The basic theory of electrostatics is related to the local net electric charge density  $\rho_e$  in the diffuse layer of EDL and charge density is coupled with the potential distribution  $\psi'$  through the Poisson-Boltzmann equation for the symmetric electrolyte is given by

$$\frac{d^2\psi'(y')}{dy'^2} = \frac{2n_0ez_v}{\epsilon} \sinh\left(\frac{ez_v\psi'(y')}{k_B T_{av}}\right) \quad \dots (3)$$

where  $n_0$  represents the concentration of ions at the bulk,  $\epsilon$  is the charge of a proton,  $z_v$  is the valence of ions,  $\epsilon$  is the permittivity of the medium,  $k_B$  is the Boltzmann constant and  $T_{av}$  is the boundary conditions for potential function are taken as

$$\begin{aligned} \psi'(y') &= \psi'_1 & \text{at } y' &= h'_1(x'), \\ \psi'(y') &= \psi'_2 & \text{at } y' &= h'_2(x'), \end{aligned} \quad \dots(4)$$

where  $\psi'_1$  and  $\psi'_2$  are the electric potential at the upper and lower wall respectively. Let us now introduce the following non-dimensional variables,





Venugopal Reddy et al.,

$$[\psi_o, \psi_1, \psi_2] = \frac{e z_v}{k_B T_{av}} [\psi', \psi'_1, \psi'_2], \quad y = \frac{y'}{d'_1} \quad \text{and} \quad x = \frac{x'}{L} \tag{5}$$

The dimensionless form of Eqs. (1) - (2) and the Poisson-Boltzmann equation defined in (3) take in the following form,

$$h_1(x) = \frac{h'_1}{d'_1} = 1 + a \cos(2\pi x), \tag{6}$$

$$h_2(x) = \frac{h'_2}{d'_1} = -d - b \cos(2\pi x + \phi), \tag{7}$$

and

$$\frac{d^2 \psi_o}{dy^2} = k^2 \sinh(\psi_o), \tag{8}$$

where  $a = \frac{a'_1}{d'_1}$ ,  $b = \frac{a'_2}{d'_1}$ ,  $d = \frac{d'_2}{d'_1}$  and  $k = \frac{d'_1}{\lambda}$  is defined as the electro-osmotic parameter,  $\lambda_2$  is the reciprocal of

the EDL thickness and is defined by  $\frac{1}{\lambda} = \left( \frac{2n_o e^2 z_v^2}{\epsilon k_B T_{av}} \right)^{\frac{1}{2}}$ . Thus the electro-osmotic parameter is inversely

proportional to EDL thickness  $\lambda$ . The dimensionless form of boundary conditions defined in (4) using the dimensionless variables (5) reduce to

$$\begin{aligned} \psi_o(y) &= \psi_1 \quad \text{at} \quad y = h_1(x), \\ \psi_o(y) &= \psi_2 \quad \text{at} \quad y = h_2(x). \end{aligned} \tag{9}$$

We assumed that the electric potential is much smaller than the thermal potential for which the Debye-Hückel linearization principle can be approximated as  $\sinh(x) \approx x$ . On the basis of this assumption, the solution of Poisson-Boltzmann equation (8) takes in the form

$$\frac{d^2 \psi_o}{dy^2} = k^2 \psi_o. \tag{10}$$

Finally, by employing the boundary conditions (9), the closed form solution of the equation (10) is given as

$$\psi_o(y) = F_1 \cosh(ky) + F_2 \sinh(ky). \tag{11}$$

**Couple Stress fluid Model**

The given set of pertinent field equations governing the flow, in laboratory frame is

$$\frac{\partial U}{\partial X} + \frac{\partial V}{\partial Y} = 0 \tag{12}$$

$$\begin{aligned} \rho \left( \frac{\partial U}{\partial t} + U \frac{\partial U}{\partial X} + V \frac{\partial U}{\partial Y} \right) &= -\frac{\partial P}{\partial X} + \mu \left( \frac{\partial^2 U}{\partial X^2} + \frac{\partial^2 U}{\partial Y^2} \right) - \eta \left( \frac{\partial^4 U}{\partial X^4} + 2 \frac{\partial^4 U}{\partial X^2 \partial Y^2} + \frac{\partial^4 U}{\partial Y^4} \right) - \sigma B_0^2 U - \frac{\mu}{k_o} U + \\ &\rho g \beta_T (T - T_0) \sin \alpha + \rho_e E \end{aligned}$$

(13)





Venugopal Reddy et al.,

$$\rho \left( \frac{\partial V}{\partial t} + U \frac{\partial V}{\partial X} + V \frac{\partial V}{\partial Y} \right) = -\frac{\partial P}{\partial Y} + \mu \left( \frac{\partial^2 V}{\partial X^2} + \frac{\partial^2 V}{\partial Y^2} \right) - \eta \left( \frac{\partial^4 V}{\partial X^4} + 2 \frac{\partial^4 V}{\partial X^2 \partial Y^2} + \frac{\partial^4 V}{\partial Y^4} \right) - \frac{\mu}{k_0} V + \rho g \beta_T (T - T_0) \cos \alpha \tag{14}$$

$$\rho c_p \left( \frac{\partial T}{\partial t} + U \frac{\partial T}{\partial X} + V \frac{\partial T}{\partial Y} \right) = k^* \left( \frac{\partial^2 T}{\partial X^2} + \frac{\partial^2 T}{\partial Y^2} \right) + Q_0 - \frac{\partial q_r}{\partial Y} + \sigma B_0^2 u^2 + \sigma E^2 \tag{15}$$

where  $(U, V)$  are the velocity components in the laboratory frame,  $\rho$  is the density,  $P$  is the pressure,  $\mu$  is the viscosity coefficient,  $\eta$  is the couple stress viscosity parameter,  $\sigma$  is the electric conductivity of the fluid,  $B_0$  is the applied transverse magnetic field,  $k_0$  is the permeability parameter,  $g$  is the acceleration due to the gravity,  $\beta_T$  and  $\beta_C$  are the coefficient of thermal and concentration expansions,  $T$  is the temperature,  $\alpha$  is the inclination angle,  $c_p$  is the specific heat at constant pressure,  $k^*$  is the thermal conductivity,  $Q_0$  is the dimensional heat absorption coefficient,  $C$  is the concentration in the reference to fixed frame system,  $D$  is the coefficient of mass diffusivity,  $K_T$  is the thermal diffusion ratio,  $T_m$  is the mean temperature,  $k_1$  is the chemical reaction parameter and  $\alpha$  is the inclination angle. The radiative heat flux in the  $X$  – direction is considered as negligible compared to  $Y$  – direction. By using Rosseland approximation for thermal radiation, the radiative heat flux  $q_r$  is specified by

$$q_r = -\frac{16\sigma^* T_o^3}{3k^*} \frac{\partial T}{\partial Y} \tag{16}$$

where  $\sigma^*$  and  $k^*$  are the Stefan-Boltzmann constant and the mean absorption coefficient respectively.

The coordinates and velocities in the wave frame  $(x, y)$  and the laboratory frame  $(X, Y)$  in a coordinate system moving with the wave speed  $c$  in which the boundary shape is stationary and are related by  $x = X - ct, y = Y, u = U - c, v = V, p(x, y) = P(X, Y, t), \bar{T}(x, y) = T(X, Y, t)$  (17)

where  $u, v$  are the velocity components,  $p$  is the pressure,  $T$  is the temperature and  $C$  is the concentration in the wave frame. Introducing the following non-dimensional quantities

$$\bar{x} = \frac{x}{\lambda}, \bar{y} = \frac{y}{d_1}, \bar{u} = \frac{u}{c}, \bar{v} = \frac{v}{c}, h_1 = \frac{H_1}{d_1}, h_2 = \frac{H_2}{d_1}, \bar{t} = \frac{ct}{\lambda}, \bar{p} = \frac{d_1^2}{\lambda \mu C} p, \delta = \frac{d_1}{\lambda},$$

$$d = \frac{d_2}{d_1}, a = \frac{a_1}{d_1}, b = \frac{a_2}{d_1}, Re = \frac{\rho c d_1}{\mu}, M = \sqrt{\frac{\sigma}{\mu}} B_0 d_1, Da = \frac{k_0}{d_1^2}, \gamma = \sqrt{\frac{\mu}{\eta}} d_1,$$

$$Gr = \frac{\rho g d_1^2 \beta_T (T_1 - T_0)}{\mu C}, \bar{\psi} = \frac{\psi}{c d_1}, Pr = \frac{\mu c_p}{k^*}, \theta = \frac{\bar{T} - \bar{T}_0}{\bar{T}_1 - \bar{T}_0}, \beta = \frac{Q_0 d_1^2}{k^* (\bar{T}_1 - \bar{T}_0)}, Sc = \frac{\mu}{\rho D},$$

$$\gamma_1 = k_1 \frac{d_1^2}{\nu}, Rd = \frac{16\sigma^* T_o^3}{3k^* \bar{\mu}_o c_f}, C_o = \frac{\left( -\frac{d\bar{p}}{d\bar{x}} \right) d_1^2}{\mu U_{HS}} \tag{18}$$





**Venugopal Reddy et al.,**

where  $\delta$  is the dimensionless wave number,  $Re$  is the Reynolds number,  $M$  is the Hartmann number,  $Da$  is the Darcy number,  $\gamma$  is the couple stress parameter,  $Gr$  is the local temperature Grashof number,  $Pr$  is the Prandtl number,  $Rd$  is the thermal radiation parameter,  $\beta$  is the heat generation parameter,  $\gamma_1$  is the chemical reaction parameter,  $Sr$  is the Soret number and  $A$  is the Joule heating parameter. Using the above transformations (17) and (18) and non-dimensional quantities (19), the governing flow field equations (13) - (15), after dropping the bars, we get

The dimensional equations of the couple stress fluid are

$$\frac{\partial^4 \psi}{\partial y^4} - \frac{1}{\gamma^2} \frac{\partial^6 \psi}{\partial y^6} - \left( M^2 + \frac{1}{Da} \right) \frac{\partial^2 \psi}{\partial y^2} + \frac{d^3 \psi_o}{dy^3} + Gr \frac{\partial \theta}{\partial y} \sin \alpha = 0 \tag{19}$$

$$\frac{(1 + Rd)}{Pr} \frac{\partial^2 \theta}{\partial y^2} + Ec \left[ \left( \frac{\partial^2 \psi}{\partial y^2} \right)^2 + \frac{1}{\gamma^2} \left( \frac{\partial^3 \psi}{\partial y^3} \right)^2 \right] + Ec M^2 \left( \frac{\partial \psi}{\partial y} \right)^2 + A = 0 \tag{20}$$

with the corresponding boundary conditions are

$$\psi = \frac{F}{2}, \frac{\partial \psi}{\partial y} + L \frac{\partial^2 \psi}{\partial y^2} = -1, \frac{\partial^3 \psi}{\partial y^3} = 0, \theta = 0 \text{ at } y = h_1 = 1 + a \cos(2\pi x) \tag{21}$$

$$\psi = -\frac{F}{2}, \frac{\partial \psi}{\partial y} - L \frac{\partial^2 \psi}{\partial y^2} = -1, \frac{\partial^3 \psi}{\partial y^3} = 0, \theta = 1 \text{ at } y = h_2 = -d - b \cos(2\pi x + \phi) \tag{22}$$

where  $L$  is the velocity slip parameter and  $F$  is the flux in the wave frame and the constants  $a, b, \phi$  and  $d$  should satisfy the relation

$$a^2 + b^2 + 2ab \cos \phi \leq (1 + d)^2. \tag{23}$$

The dimensionless mean flow rate  $\Theta$  in the fixed frame is related to the non-dimensional mean flow rate  $F$  in wave frame by

$$\Theta = F + 1 + d \tag{24}$$

and in which

$$F = \int_{h_1}^{h_2} \frac{\partial \psi}{\partial y} dy \tag{25}$$

**Numerical Solution**

The solution of system of coupled non-linear Eqs. (20) - (22) with corresponding boundary conditions in Eq. (23) - (24) are obtained using NDSolve in Mathematica computational software. This section contains the plots and related analyses for different embedded parameters. This section includes the graphs for velocity, temperature, concentration and pressure gradient.





### Velocity distribution

Fig. 2 displays the velocity profile for various values of Hartmann number. The velocity decreases and drops with Hartmann number  $M$ . Fig. 3 depicts velocity profiles of different values of parameter for osmosis parameter. Velocity profile is seen to raise as osmosis parameter  $k$  enlarges. Fig. 4 depicts that the consequences of the parameter  $\lambda_1$  on the profile of velocity. It is clear that enhance the strength of  $\lambda_1$  resulted in enhancing the velocity. Fig. 5 indicate that the velocity rises with increasing  $Da$ . Fig. 6 reveals that velocity is seen to decrease with the higher values of couple stress parameter. Fig. 7 shows that velocity diminishes with increasing  $L$ .

### Temperature distribution

Fig. 8 – 11 depicts the deviations in temperature profiles for various values of parameters  $A$ ,  $k$ ,  $Ec$  and  $Pr$ . Fig. 8 presents the consequences of the parameter  $A$  on the profile of temperature. It is clear that enhance the strength of  $A$  resulted in increasing the temperature. Fig. 9 shows that temperature rises with enhancing  $k$ . Fig. 10 shows that the temperature enhances significantly with a rise in  $Ec$ . Fig. 11 shows a very significant effect of  $Pr$  on the temperature profiles. It is clear from this figure that the Brinkman number has a impulse to diminish the temperature in the micro-channel. It may be inferred that the thermal conductivity of the fluid declines by enhancing the ratio of momentum diffusivity to thermal diffusivity.

### Pumping characteristics

Figs. 13 - 15 represent the profiles of pressure gradient  $\left(\frac{dp}{dx}\right)$  for the effects of Slip parameter ( $L$ ), Osmosis parameter ( $k$ ) and the couple stress parameter ( $\gamma$ ). The pressure gradient has oscillatory behavior in the whole range of the x-axis. From all figures, it is clear that the pressure gradient diminishes with the higher values of  $L$ ,  $k$  and  $\gamma$ . The pressure rise is a significant physical measure in the peristaltic mechanism. The results are prepared and discussed for different physical parameters of interest through Figs. 16 – 18 and which are plotted for dimensionless pressure rise  $\Delta P_\lambda$  versus the dimensionless flow rate  $\Theta$  to the effects of Hartmann number  $M$ , chemical reaction parameter  $\gamma_1$ , heat generation parameter  $\beta$  and couple stress parameter  $\gamma$ . The pumping regions are peristaltic pumping ( $\Theta > 0, \Delta P_\lambda > 0$ ), augment pumping ( $\Theta < 0, \Delta P_\lambda < 0$ ), retrograde pumping ( $\Theta < 0, \Delta P_\lambda > 0$ ), co pumping ( $\Theta > 0, \Delta P_\lambda < 0$ ) and free pumping ( $\Theta = 0, \Delta P_\lambda = 0$ ). Fig. 16 is depicted that the pressure rise  $\Delta P_\lambda$  depressing with an enhance in Hartmann number  $M$  in the both peristaltic pumping region and free pumping region. Fig. 17 depicts that the quite opposite nature that of for the effect of the heat generation parameter  $\beta$ . The influence of couple stress fluid parameter  $\gamma$  on the pressure rise is decreases and which is elucidated from Fig. 18.

### Nusselt number

Figs. (19) – (21) exhibits the influence of incorporated parameters such as Hartmann number  $M$ , Osmosis parameter  $k$  and Joule heating parameter  $A$  respectively on magnitude of Nusselt number. The heat transfer coefficient has oscillatory in nature due to peristaltic motion of walls. The heat transfer rate enhances for  $M$ ,  $k$  and  $A$  from Figs. 19 - 21.





### Venugopal Reddy *et al.*,

#### Sherwood number

The mass transfer coefficient shows the impact of different parameters of  $\lambda_1$  and  $k$  from Figs. 22 – 23. Fig. 22 depicts the Sherwood number depresses with the impact of  $\lambda_1$  whereas it observes the mass transfer coefficient enhances as the parameter  $k$  rises from Fig. 23.

#### Trapping Phenomenon

The phenomenon of trapping in flow of fluid is trapping and is presented by drawing streamlines in the Figs. 24 - 27. A bolus is having by splitting of a streamline under important conditions and it is followed along with the wave in the wave frame. This process is called trapping. The bolus of trapping is observed to expand by enhancing  $M$  from Figs. 24 – 25. However the size of bolus decreases by the rising effects of  $\lambda_1$  as shown in Figs. 26 – 27.

#### Concluding Remarks

We have investigated the peristaltic transport of a heat and mass transfer of couple stress fluid on the combined impacts of electro-osmotically and pressure driven flow in an inclined asymmetric micro channel whose walls are varying sinusoidally with different wave trains. Effects of thermal radiation, chemical reaction and Joule heating have been accounted. The numerical solution for velocity, temperature distribution, concentration distribution and pumping characteristics are presented using small wave length and small Reynolds number. The important findings of present study are summarized as follows

- The Electro – osmotic flow of couple stress fluids in an inclined asymmetric channel is strongly depend on Debye length.
- Velocity diminishes with an enhance of  $L$  and  $\gamma$ .
- Temperature rises with an strength of  $A$  where as depresses with an enhance of  $Rd$ .
- It is observed that pressure gradient has oscillatory behavior.
- Pressure rise decreases with an effect of increasing  $\gamma$
- The absence of Electro – Osmosis, our results are in good agreement with Gnaneswara Reddy *et al.* [33].

#### REFERENCES

1. K.P. Tikhomolova, Electro-Osmosis, Ellis Horwood, London, 1993.
2. H. Ginsburg, Analysis of plant root electro-potentials, J. Theor. Biol. 37 (1972) 389 – 412.
3. V. Sansalone, J. Kaiser, S. Naili, T. Lemaire, Interstitial fluid flow within bone canaliculi and electro-chemo-mechanica features of the canalicular milieu, Biomech. Model. Mechanobiol. 12 (2013) 533 – 553.
4. E.A. Marshall, The osmotic flow of an electrolyte through a charged porous membrane, J. Theor. Biol. 66 (1977) 107 – 135.
5. S. Grimnes, Skin impedance and electro-osmosis in the human epidermis, Med. Biol. Eng. Compu. 21 (1983) 739 – 749.
6. T.A. Davis, Electrodialysis, in: M.C. Porter (Ed.), Handbook of Industrial Membrane Technology, Noyes Publications, New Jersey, USA, 1990.
7. V. Orsat, G.S.V. Raghavan, E.R. Norris, Food processing waste dewatering by electro- osmosis, Can. Agric. Eng. 38 (1996) 063 – 067.
8. A. Manz, C.S. Effenhauser, N. Burggraf, D.J. Harrison, K. Seiler, K. Fluri, J. Micromech. Microeng. 4 (1994) 257.
9. G.D. Ngoma, F. Erchiqui, Pressure gradient and electroosmotic effects on two immiscible fluids in a microchannel between two parallel plates, J. Micromech. Microeng. 16 (2005) 83 – 90.
10. T.S. Zhao, Q. Liao, Thermal effects on electro-osmotic pumping of liquids in microchannels, J. Micromech. Microeng. 12 (2002) 962.





**Venugopal Reddy et al.,**

11. A. Mondal and G.C. Shit, Heat transfer analysis on electro-osmotic flow in a slowly varying asymmetric micro-channel, *European Journal of Mechanics-B/Fluids*, 60 (2016) 1 - 35.
12. VK. Stokes, Couple stresses in fluids, *Phys Fluids*, 9 (1966) 1709 – 15.
13. M. Devakar, V. Iyengar, Stokes problems for an incompressible couple stress fluid, *Nonlinear Anal Model Control* 2008:181 – 90.
14. JS Duan, X Qui, Stokes second problem of viscoelastic fluids with constitutive equation of distributed-order derivative. *Appl. Math. Comput.* 331(2018)130 – 9.
15. K. Ramesh, Influence of heat and mass transfer on peristaltic flow of couple stress fluid through porous medium in the presence of inclined magnetic field in an inclined asymmetric channel. *J. Mol. Liq.* 219 (2016) 256 – 71.
16. A. Alsaedi, N Ali, D.Tripathi, T. Hayat, Peristaltic flow of couple stress fluid through uniform porous medium. *Appl Math Mech.* 35 (2014) 469 – 80.
17. K. Kaladhar, Natural convection flow of couple stress fluid in a vertical channel with Hall and Joule heating effects. *Proc.Eng.* 127 (2015) 1071 – 8.
18. T. Hayat, M. Iqbal, H Yasmin, F Alsaedi. Hall effects on peristaltic flow of couple stress fluid in an inclined asymmetric channel. *Int. J. Bio mathematics*, 7(2014)1450057(34pages).
19. T.W. Latham, *Fluid motion in a peristaltic pump*, MIT Press, Cambridge Mass, USA.
20. A.H. Shapiro, M.Y. Jaffrin, and S.L. Weinberg (1969), Peristaltic pumping with long wavelengths at low Reynolds numbers, *J. Fluid Mech.*, 37 (1969) 799–825.
21. Mekheimer Kh.S., and Elmaboud Y.A., Peristaltic flow of a couple stress fluid in an annulus application of an endoscope. *Physica A*, Vol. 387, pp. 2403–2415.
22. O.D., Makinde, and P.Y. Mhone (2006), Hydromagnetic effects on internal flow separation in a diverging channel, *Romanian Journal of Physics*, Vol. 51, pp. 959-966.
23. Hayat T., Javed M., and Ali N., (2008), MHD peristaltic transport of Jeffrey fluid in a channel with compliant walls and porous space, *Transp. Porous Media*, Vol. 74, pp. 259–274.
24. Mekheimer Kh.S., and Abd elmaboud Y., (2008), Peristaltic flow of a couple stress fluid in an annulus: application of an endoscope, *Physica A*, Vol. 38, pp. 2403–2415.
25. Adesanya S.O., and Makinde O.D., (2012), Heat transfer to magneto hydrodynamic non-Newtonian couple stress pulsatile flow between two parallel porous plates, *Zeitschrift for Naturforschung* , Vol. 67a, pp. 647 – 656.
26. Adesanya S.O., and Makinde O.D., (2015), Irreversibility analysis in a couple stress film flow along an inclined heated plate with adiabatic free surface, *Physica A*, Vol. 432, pp. 222-229.
27. Ganeswara Reddy M., and Venugopal Reddy K., (2016), Impact of velocity slip and joule heating on MHD peristaltic flow through a porous medium with chemical reaction, *Journal of the Nigerian Mathematical society*, Vol. 35, pp. 227 - 244.
28. M. Ganeswara Reddy, K. Venugopal Reddy, and O.D. Makinde, Hydromagnetic peristaltic motion of a reacting and radiating couple Stress fluid in an inclined asymmetric channel filled with a porous medium, *Alexandria Engineering Journal*, 55 (2016) 1841–1853.
29. M. Mishra, and A. R. Rao, Peristaltic transport of a Newtonian fluid in an asymmetric channel, *Z. Angew. Math. Phys.*, 53 (2003) 532 - 550.
30. M. Kothandapani, and S. Srinivas, Peristaltic transport of a Jeffrey fluid under the effect of magnetic field in an asymmetric channel, *Int. J. Nonlinear Mech.*, 43 (2008) 915–924.
31. F. M. Abbasi, T. Hayat, B. Ahmad, and B. Chen, (2015), Peristaltic flow with convective mass condition and thermal radiation, *J. Cent. South Univ.*, 22 (2015) 2369–2375.
32. M. Ganeswara Reddy, K. Venugopal Reddy, and O.D. Makinde, (2016) Hydromagnetic peristaltic motion of a reacting and radiating couple Stress fluid in an inclined asymmetric channel filled with a porous medium, *Alexandria Engineering Journal*, 55 (2016) 1841 - 1853.
33. M. Ganeswara Reddy, K. Venugopal Reddy, and O.D. Makinde, Heat transfer on MHD peristaltic rotating flow of a Jeffrey fluid in an asymmetric channel, *International Journal of Applied and Computational Mathematics*, DOI 10.1007/s40819-016-0293-1 (2016).

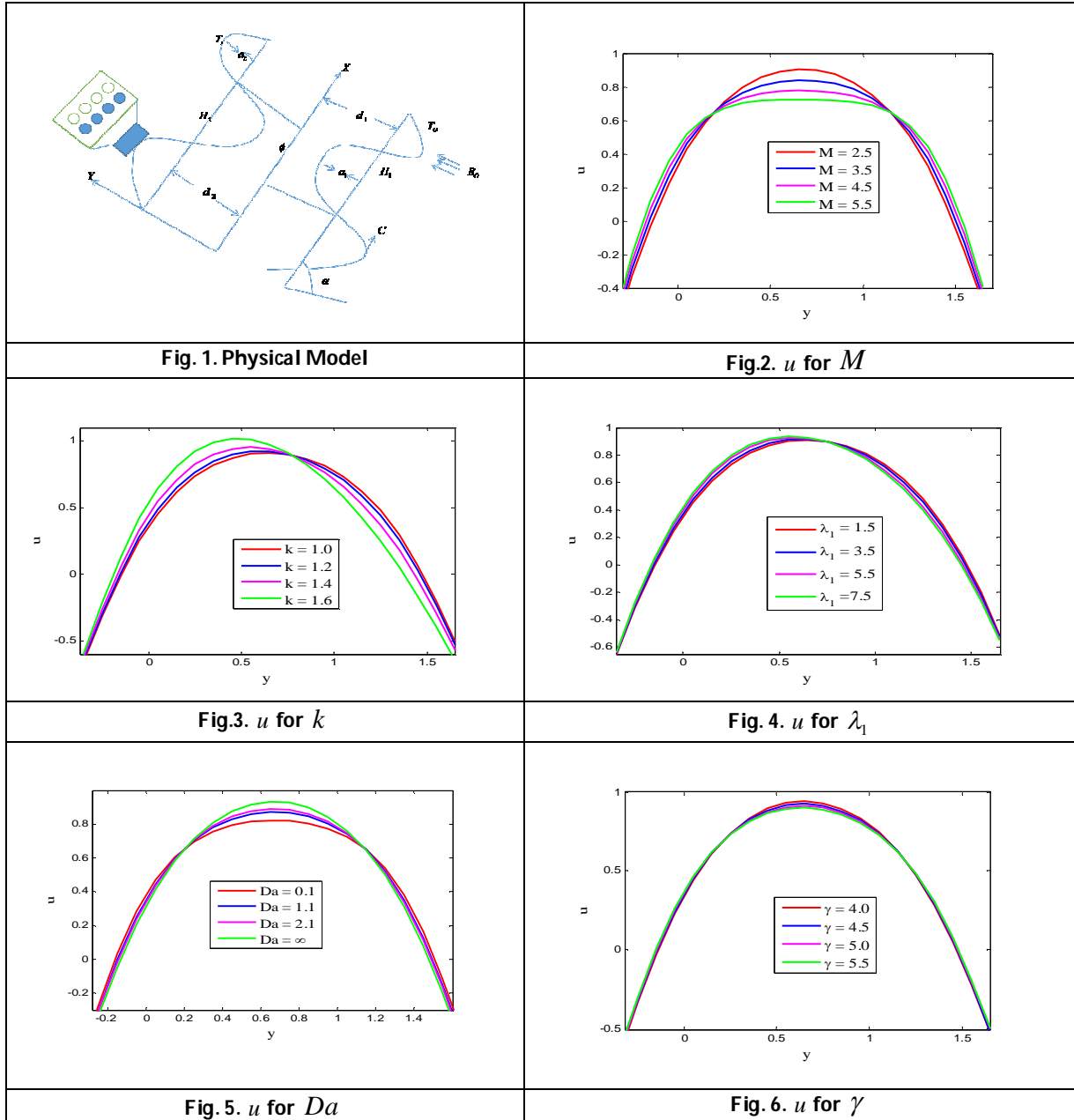


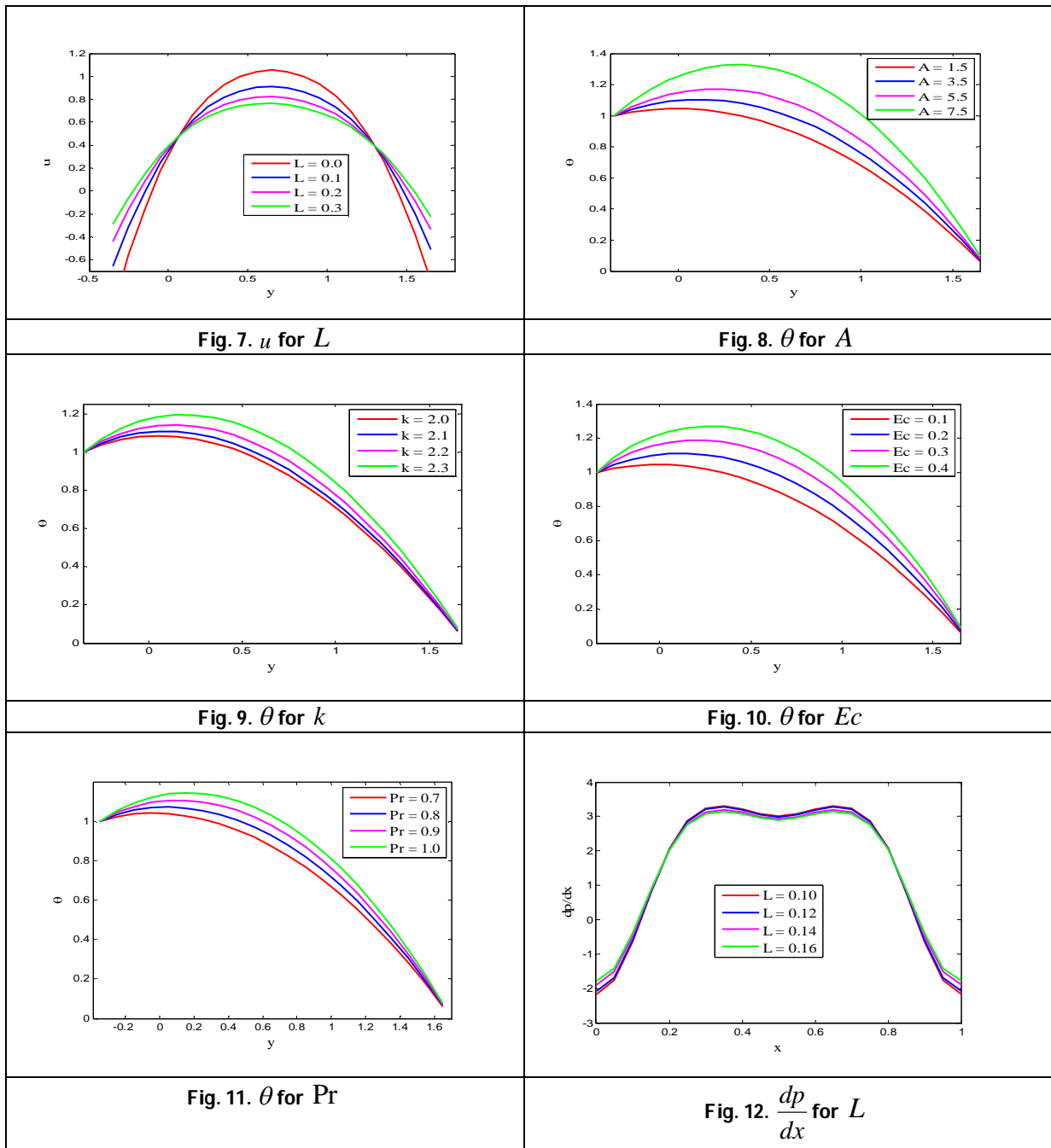




Venugopal Reddy et al.,

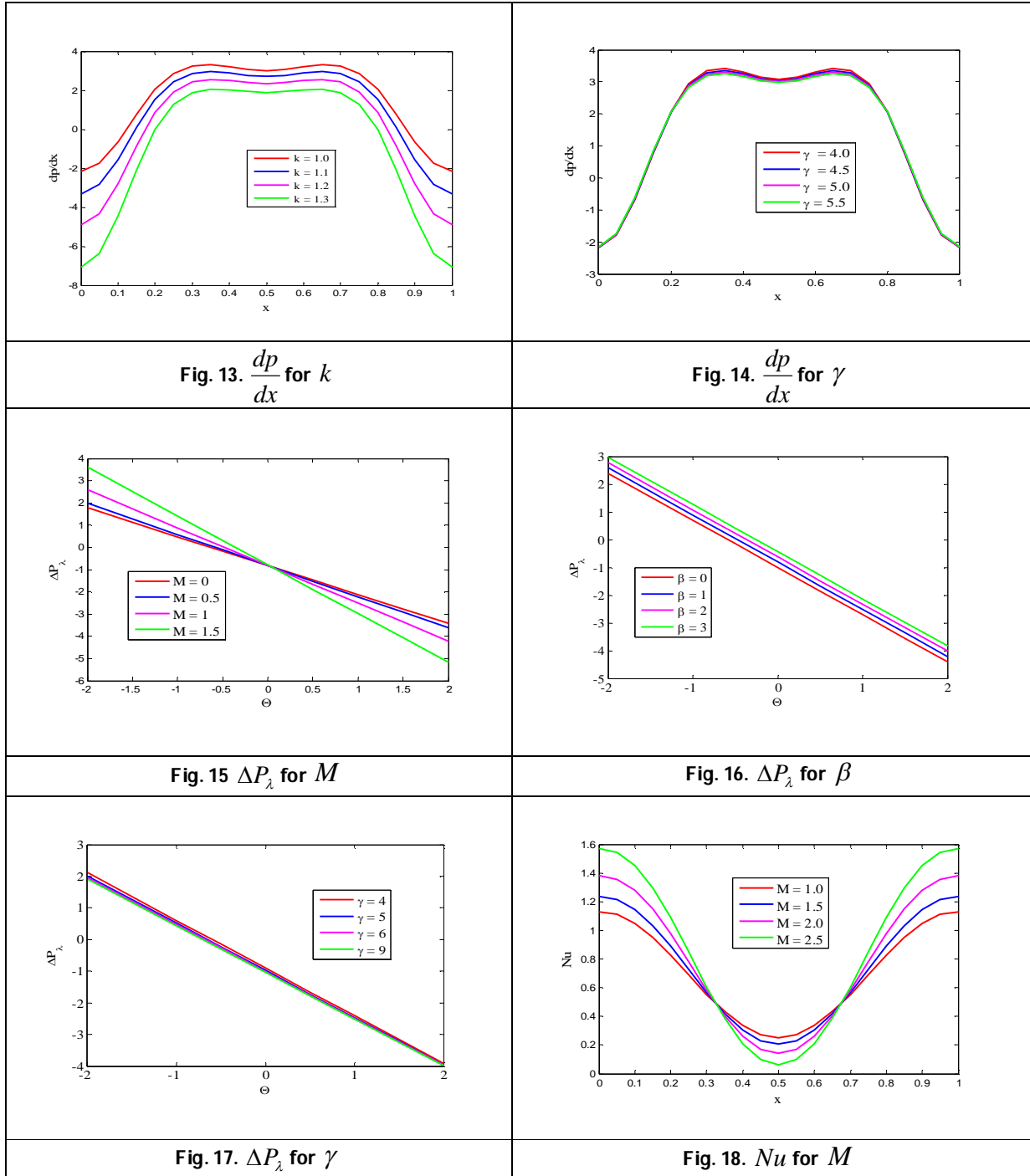
34. O.D. Makinde, M. Gnaneswara Reddy, and K. Venugopal Reddy, Effects of thermal radiation on MHD peristaltic Motion of Walters-B Fluid with heat source and Slip conditions, Journal of Applied and Fluid Mechanics, 10(2017)1105-1112.







**Venugopal Reddy et al.,**



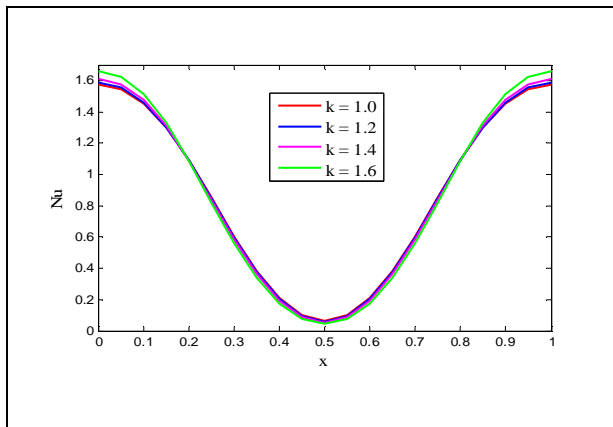


Fig. 19. Nu for  $k$

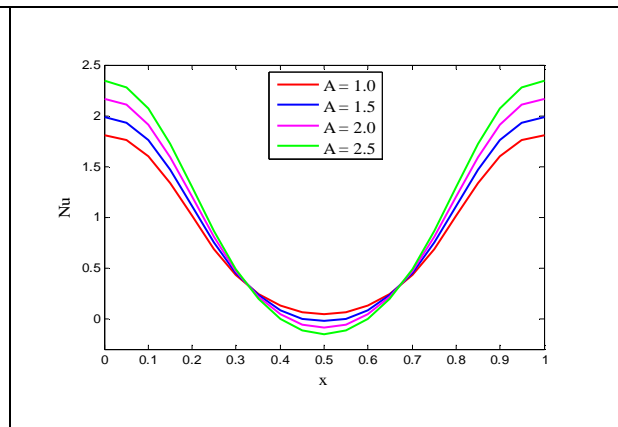


Fig. 20. Nu for  $A$

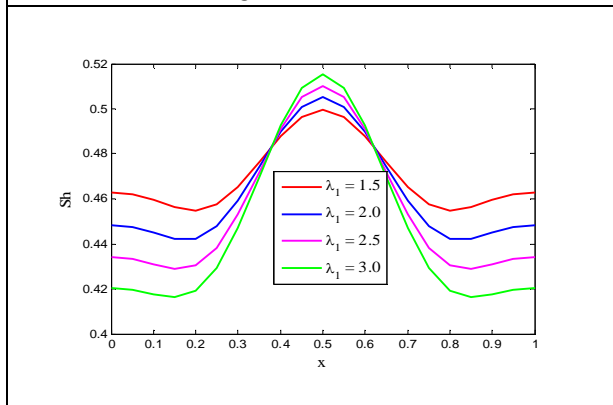


Fig. 21.  $Sh$  for  $\lambda_1$

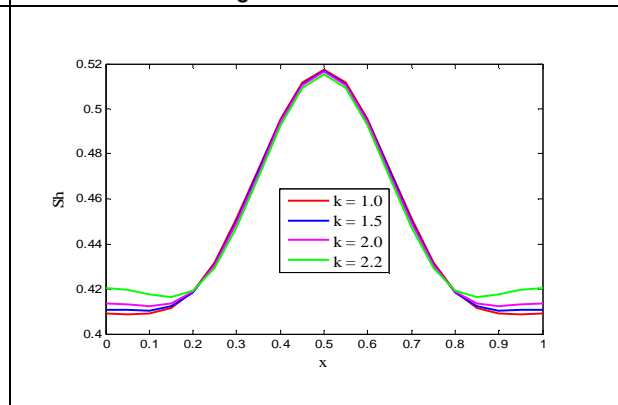


Fig. 22.  $Sh$  for  $k$

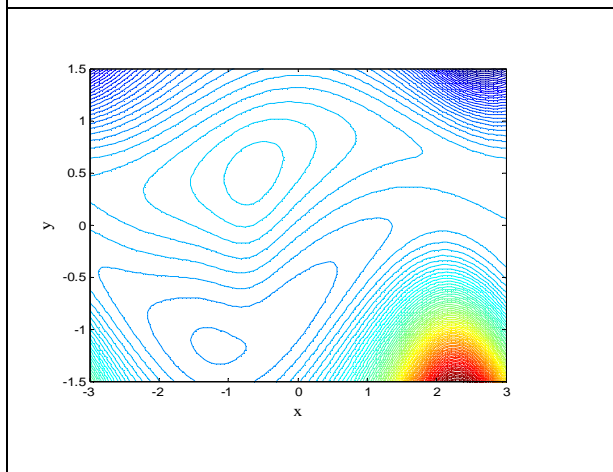


Fig. 23. Effect of  $M$  on stream lines for  $M = 1.5$ .

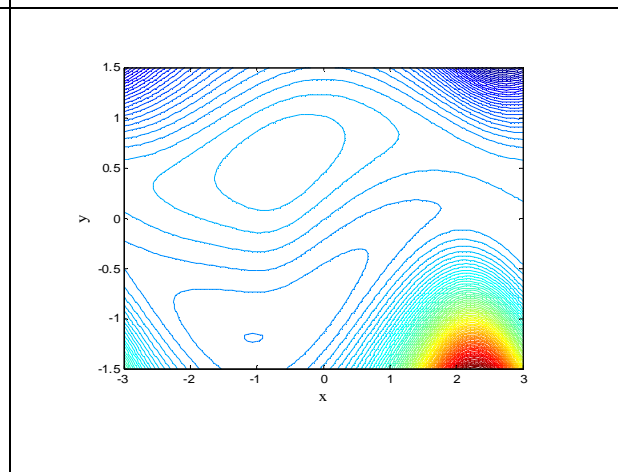


Fig.24. Effect of  $M$  on stream lines for  $M = 1.6$ .





Venugopal Reddy et al.,

